Innovative: International Multi-disciplinary Journal of Applied Technology
(ISSN 2995-486X) VOLUME 02 ISSUE 12, 2024

Analysis of Aluminium Anodization Process; Impact of Operation Variables, And Morphology Study

Muataz Mohammed Sulaiman [1], Falah K. Matloub [2],
Sata Kathum A. Ajjam [1], Hameed Hussein Alwan [1]
[1] University of Babylon/ Chemical Engineering Department, Iraq,
[2] University of hilla/ Department of refrigeration and air conditioning engineering technologies, Iraq

Abstract:

This work is to construct anodic aluminium oxide layer by anodization. the anodization process was done by immersed aluminium specie in sulfuric acid solution with three different concentrations; 12, 15, and 18 wt.%, in which the study consists of investigation the impact temperature, time and current density. The morphology, growth, and chemical composition of layer by characterize was done by Energy dispersive X-ray (EDS), scanning electronic microscope (SEM), and X-ray diffraction (XRD).

Anodizing was done by varying the temperature at range 20°C to 30 °C, anodization time from 25 to 35 minutes, and the current density from 2 to 3 μA/cm2. The results show that the weight gain ranged between 0.0229 to 0.125 g, and it was increased with temperature and anodization time, while it was decrease with acid concentration. The layer thickness was decreased with temperature, while it is increased with current density, acid concentration and time, but it decreased with temperature. DS investigation show that the average ration of Oxygen/Aluminium (O/Al) between 1.096 and 1.307 which depended on electrolyte.

Keywords: Anodization, anodized oxide layer, porous anodized layer.

Introduction

Anodization is an electrochemical method used as a surface treatment to improve the thickness and characteristics of the oxide layer formed on certain metals, such as aluminium, thereby improving corrosion resistance. Aluminium and its alloys are of significant interest among metals due to their considerable commercial value in industry [1]. Anodic oxide layers are generated during the anodization of metals, serving as one of the most effective conversion coatings for protecting metals in corrosive environments. It also enhances the appearance of the aluminium surface. This technology has significantly enhanced the processing of aluminium and aluminium alloys. The features of the anodic oxide layer render aluminium goods suitable for a diverse array of applications, including architectural, packaging, and aerospace sectors [2].

The significant increase in hardness of the anodic coating compared to non-anodized aluminum facilitates maintenance and cleaning procedures. Sulphuric acid is used to make anodic oxide layers. Anodizing aluminium with sulphuric acid creates a porous layer with a central pore that is orientated vertically to the aluminium substrate. This layer is made up of closely packed columnar hexagonal units. The depth of the barrier layer and pore diameter correlate with the applied voltage and operating temperature, whereas the height of the pore or thickness of the porous film increases with time. The anodic oxide film is optically clear; however, when the layer is porous, it transforms into a highly adsorbent layer, making it appropriate for colouring. Interference colouring is an intriguing approach that provides a diverse spectrum of hues using a very inexpensive method employed in many applications[3].

Aluminium anodization is categorised into two operational groups: mild (soft) anodization (MA) and hard (tough) anodization (HA). The MA operation produces linear and organised nanopores; nevertheless, it is not rapid and can only be utilised within a limited range of operational circumstances. The HA operation was initially created in the surface termination sector and has been widely employed for other industrial applications. The current density for the (HA) type is usually 1-2 orders of magnitude higher than that for the (MA) type. This means that the anodized oxide layer grows 25–35 times faster in the HA type than in the MA type. Nonetheless, HA forms a disordered oxide layer, and the irregular pore structure contains micrometre-sized fissures. To resolve this issue, it was proposed that a thin protective oxide coating be formed on the aluminium surface before commencing HA operation. The significant increase in hardness of the anodic coating compared to non-anodized aluminum facilitates maintenance and cleaning procedures. Sulphuric acid is used to make anodic oxide layers. Anodizing aluminium with sulphuric acid creates a porous layer with a central pore that is orientated vertically to the aluminium substrate. This layer is made up of a dense array of columnar hexagonal units. The pore diameter and depth of the barrier layer are dependent on the operating temperature and applied voltage, whereas the height of the pore or thickness of the porous film increases with time. The produced anodic oxide film is optically clear, but when the layer is porous, it transforms into a highly adsorbent layer, making it excellent for colouring. Interference colouring is an intriguing approach that provides a diverse spectrum of hues using a very inexpensive method employed in many applications[4].

Anodizing is a surface treatment that is advantageous for aluminium alloys and improves performance, including corrosion resistance, adherence of polymer layers, and wear resistance. Anodized aluminium oxide layers consist of a thin, dense interior film and a thick, porous exterior coating. This layer consists of a hexagonal columnar unit structure with a single pore located at the hexagonal unit's core. Post-anodizing treatments are necessary to seal the pores and fill the exterior with a with a thick, porous layer to enhance corrosion resistance, hardness, wear resistance, and aesthetic appearance. The predominant sealing techniques employed in the industrial sector include steam, boiling water, nickel acetate, dichromate, and cold nickel fluoride sealing, among others. While typical sealing techniques enhance corrosion resistance, they inadequately influence mechanical qualities, including hardness and wear resistance. To date, electrolysis conditions, including applied electric power, temperature, and electrolyte composition, have been investigated to improve the mechanical characteristics of oxide films [5].

The efficacy of the anodic layer is often regarded as contingent upon its structure and is affected by several factors, including additives, current density, and electrolyte type. Direct current anodizing is a prevalent electrochemical technique utilised to generate an oxide layer. Nevertheless, a significant limitation of this approach is the generation of a substantial volume proportion of voids at the cell edges. It has been demonstrated that the mechanical capabilities of anodized coatings may be reduced by the presence of such a porous structure. The oxidation of O ions on the surface of the AAO layer results in the generation of oxygen gas bubbles, which is responsible for the formation of these gaps. It is assumed that the gas bubbles generate a gaseous layer on the coating's surface, which in turn raises the temperature of the anodic layer as a result of the substantial thermal conductivity difference between the gas bubbles and the porous layer. The mechanical and corrosion resistance of the coating is reduced as a result of an increase in thermal content or temperature on the surface of the AAO layer, which affects the anodized layer's development, structure, and dissolution[6].

Experimental Work

Experimental methods and instrumentations used for anodization process are comprised. The solutions, specimens' preparation, and the electrochemical cell are mentioned.

Chemicals:

The chemical formula, purity, and manufacturer of the substances utilised in this study are presented in Table 1.

Table -1: The chemicals used in the work

Materials	Chemical formula	Purity	Manufacturer
Nitric acid	hno_3	65	Thomas Baker, India
Sulphuric acid	h_2so_4	98	SDFCL, India
Sodium hydroxide	NaOH	99	Thomas Baker, India

Experiment sequences:

The specimens were first treated with an alkaline solution of 60 g/l NaOH at 60 °C for two to three minutes. They were then immersed in 30 to 50 vol% HNO3 at ambient temperature for 60 seconds, and they were washed well with deionised water. The specimens experienced anodization in a 15 wt.% sulphuric acid solution for 30 minutes at current densities of 2, 2.5, and 3 $\mu A/cm^2$. The electrolyte temperature range was 20, 25, and 30 °C. Subsequent to anodizing, the specimens were washed with deionised water and promptly submerged in a 4% dye solution for colouring before being dried.

Specimen Preparation:

Aluminium alloy sheets measuring 100 x 7 x 0.8 mm were utilized as substrates for anodizing processes. Specimen were abraded in sequence by SiC papers of the following grades (100, 200, 400, 600) under running tap water and dried with tissue paper, then immersed in ethanol for (1-2) minute and dried with tissue paper. The dimensions of specimen were measured with a vernier to the 2nd decimal of millimetre.

The Electrochemical Cell:

Rectangular batch electrochemical cell consists of aluminium anode and two cathodes. The cathode and anode are separated by 20 millimetres. The immersed length of electrodes is 50mm. The anode electrode weighed before the immersion in NaOH solution and after drying. Aluminium sheets were cut into rectangular samples of (1.5 × 2 × 0.05) cm, which were utilized as both cathode and anode. The samples were pretreated by washing with acetone and rinsed with distilled water to remove oil, grease and general dirt. The samples were etched by immersing them in a 5% sodium hydroxide solution at 45°C for 5 minutes, followed by rinsing with tap water and subsequently with distilled water. The electrolyte temperature is set to specified values of 20, 25, and 25 °C, with immersion times of 25, 30, and 35 minutes, and current densities of 2, 2.5, and 3 $\mu A/dm^2$. The sample was rinsed with running water post-electropolishing, subsequently with distilled water, dried, and then preserved in a desiccator containing silica gel before weighing (W1). 4. Configure the anodising cell in accordance with the equipment depicted in Fig. 1. The sample was immersed in an anodising cell containing 12%, 15%, and 18% $H2SO4$ solution, after anodizing, it was dried in a drying oven and weighed (W2). Rinsed the sample with water, followed by distilled water, then dried and weighed (W3). The thickness of the anodic film is determined using the following equation:

$$T\ (\mu m) = \frac{(W_2 - W_3)\times 10^4}{S\rho}$$

Where:

T is thickness of the anodized layer (micron).

W2 is weight of a sample with anodic layer (grams).

W3 is weight of a sample post-stripping (grams).

S is surface are (dm$^{3)}$.

ρ is density (g / cm^3).

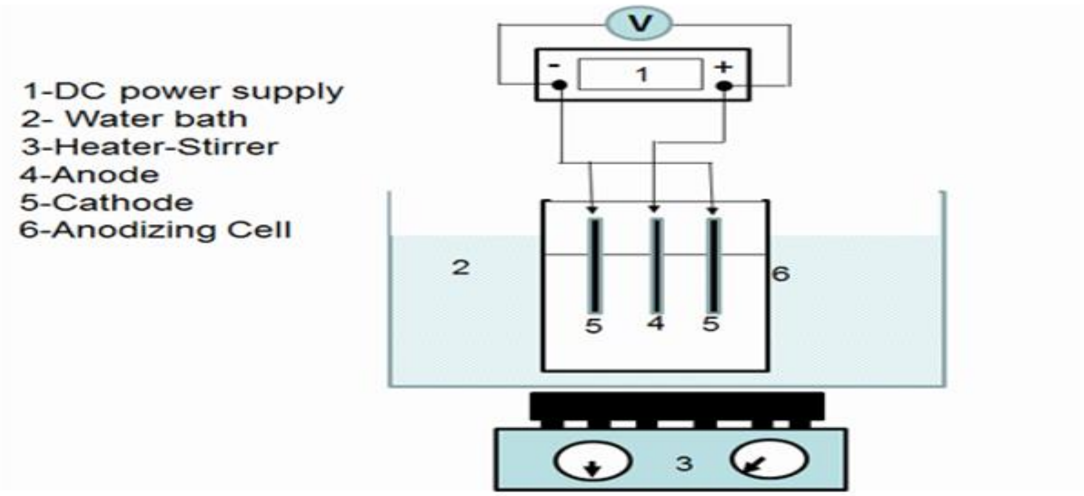

Figure 1: anodizing cell apparatus

The anodized layer was characterized by X-ray diffraction (XRD), and Energy dispersive X-ray (EDX), while the morphology for the anodized layer was investigated by scanning electronic microscopic (SEM).

Results and discussion

Anodized layer characterization

Table-2: Characterization for the four samples were prepared under the following conditions.

Sample	Current density (μA/cm^2)	Anodization temperature (°C)	Anodization time (min.)	H2SO4 concentration
S1	2.5	25	30	18%
S2	3	25	30	18%
S3	2.5	25	35	12%
S4	2.5	25	30	15%

X-Ray diffraction (XRD)

In this study, XRD analysis was employed to obtain a comprehensive understanding the effect of anodizing conditions, as seem in **Fig.2** the diffraction peak for anodized aluminium sample in

H_2SO_4 solution, there are three sharp peaks in which γ – aluminium oxide (γ –Al_2O_3) was formed on the aluminium surface. The peaks at 2θ angle around 44. 74 ° (JCPDS# 47-1308), 63.11° (JCPDS# 29-0063), and 78.07° (JCPDS#04-0877) and these findings align harmoniously with the anticipated composition and corroborating the existence of γ –Al_2O_3 [7] , and [8]. A note worth mentioning is the distinctive peak 2θ =63.11° at the corner in S1, which was worked on at a temperature of 30 °C while another sample (S2, S3 and S4) done at 25 °C. The influence of temperature on oxide layer development is evident, as it impacts the rate of ion transfer across the oxide layer, the rates of heat transfer within the pores and the electrolyte solution, and the dissolution of the oxide from the pore wall[9].

Energy dispersive X-ray (EDX)

The EDX analysis results of the elemental composition of the anodized aluminium samples are presented in **Figs. 3-6** , the findings confirm the successful integration oxygen and aluminium at Al_2O_3 form, and this is consistent with the analysis of XRD, as well as the EDX mapping analysis confirms the presence of sulfur in these samples. The disparity between the expected theoretical loadings and the detected percentages can be attributed to various factors. This small discrepancy can be attributed to the observation that the measured percentages represent the catalyst's surface composition, which may vary somewhat from its bulk composition. Contamination, surface oxidation, or the adsorption of additional elements may account for the discrepancies between the predicted and measured values. As noted in Fig. the average oxygen content of the sample s1 is 40.76% (yellow0), while the aluminium content is 34.25% (red). The close to these values can be seen for other samples; 40.95%, and 37.37 % for oxygen and aluminium respectively in sample S2, furthermore there are 42.65 %, and 34.19 % for oxygen, and aluminium respectively in sample S3. Finely they are 43.30, and 35.19 for oxygen, and aluminium respectively in sample S4. The EDS test showed what chemicals were in the anodized oxide layer. It showed that the oxygen-to-aluminium (O/Al) ratio goes down as the temperature rises and the number of aluminium increases slightly. The average O/Al ratio ranged from 1.096 to 1.307, contingent upon electrolyte concentration. Sulphur was also identified in the oxide layer.

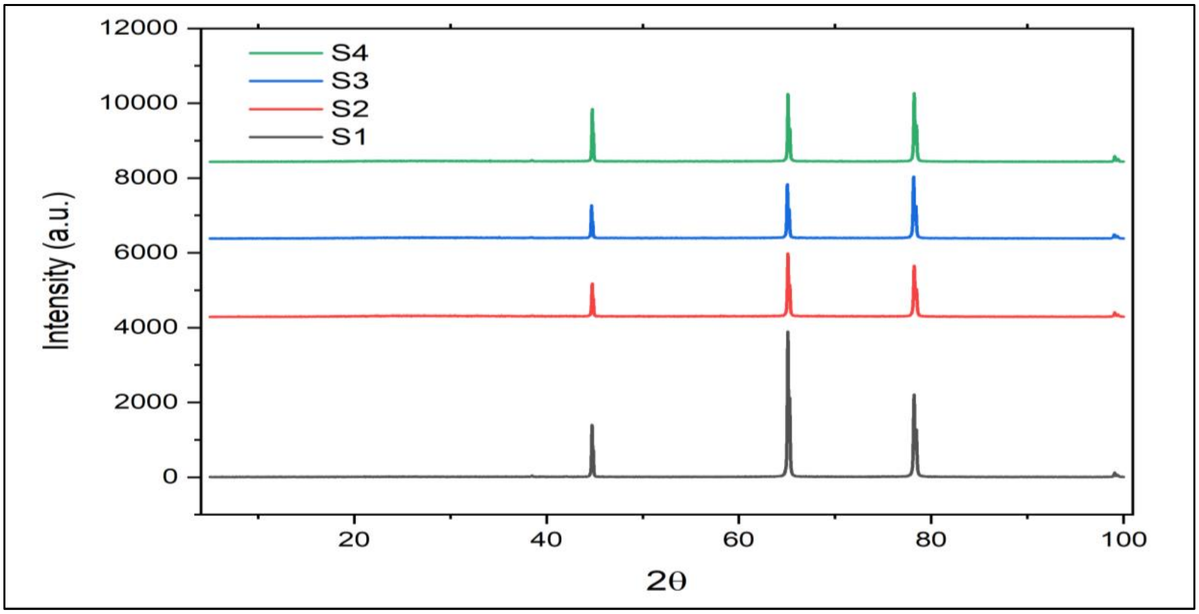

Figure 2: X-ray diffraction patterns for anodized samples S1, S2, S3, and S4.

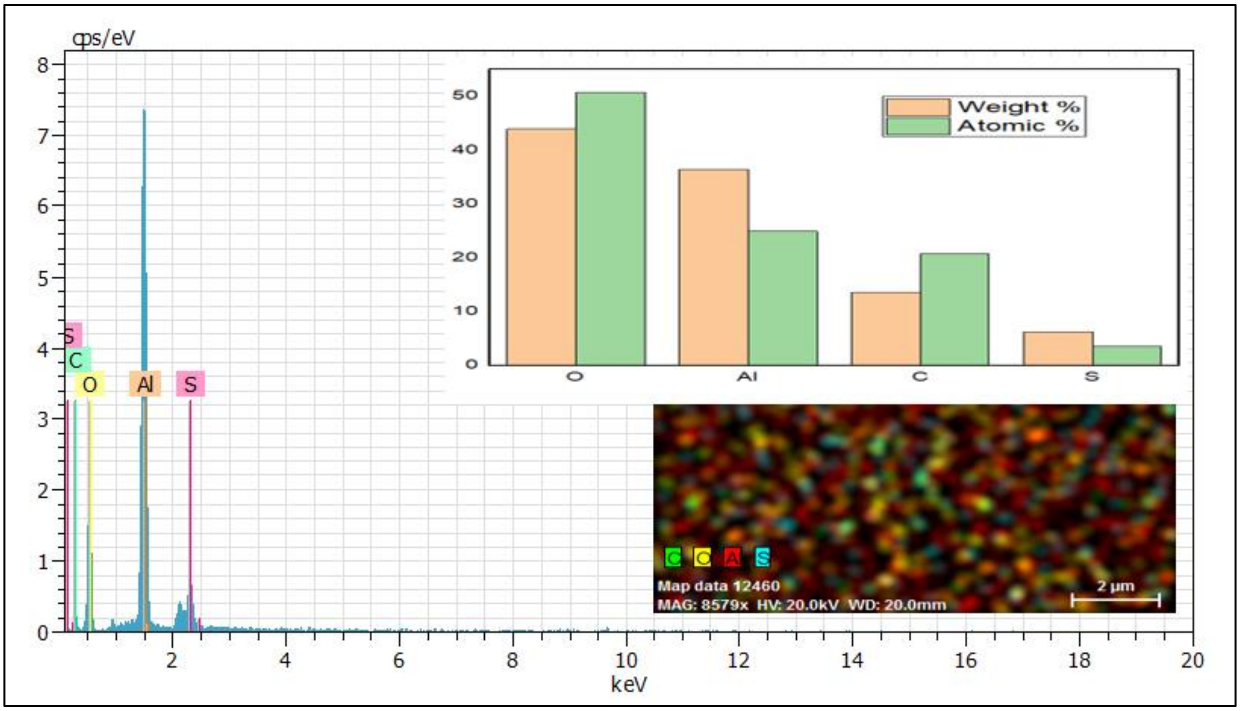

Figure -3: The chemical composition of the sample S1

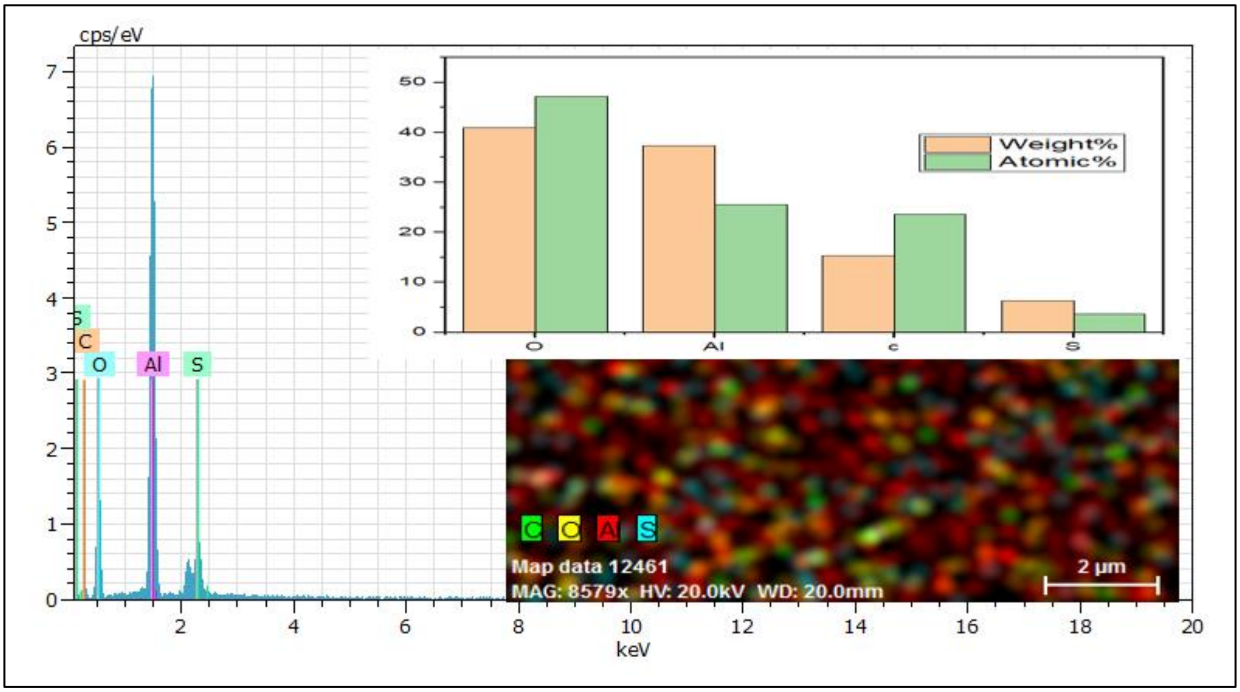

Figure-4: The chemical composition of the sample S2

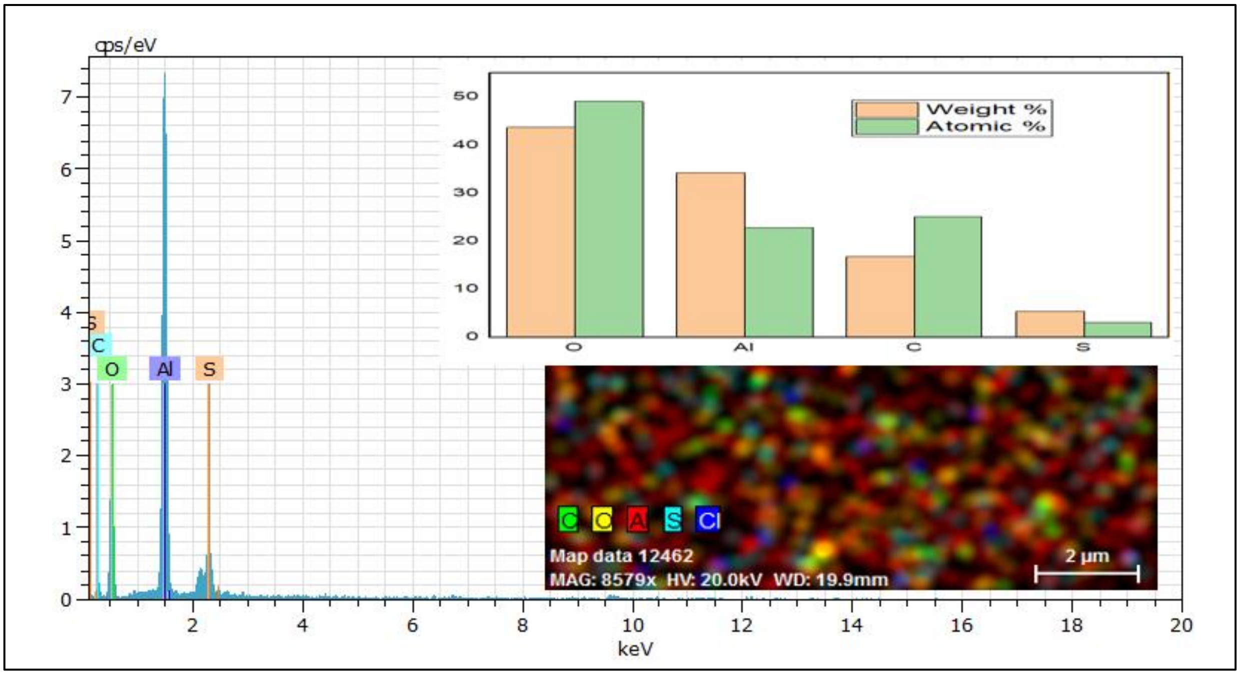

Figure -5: The chemical composition of the sample S3

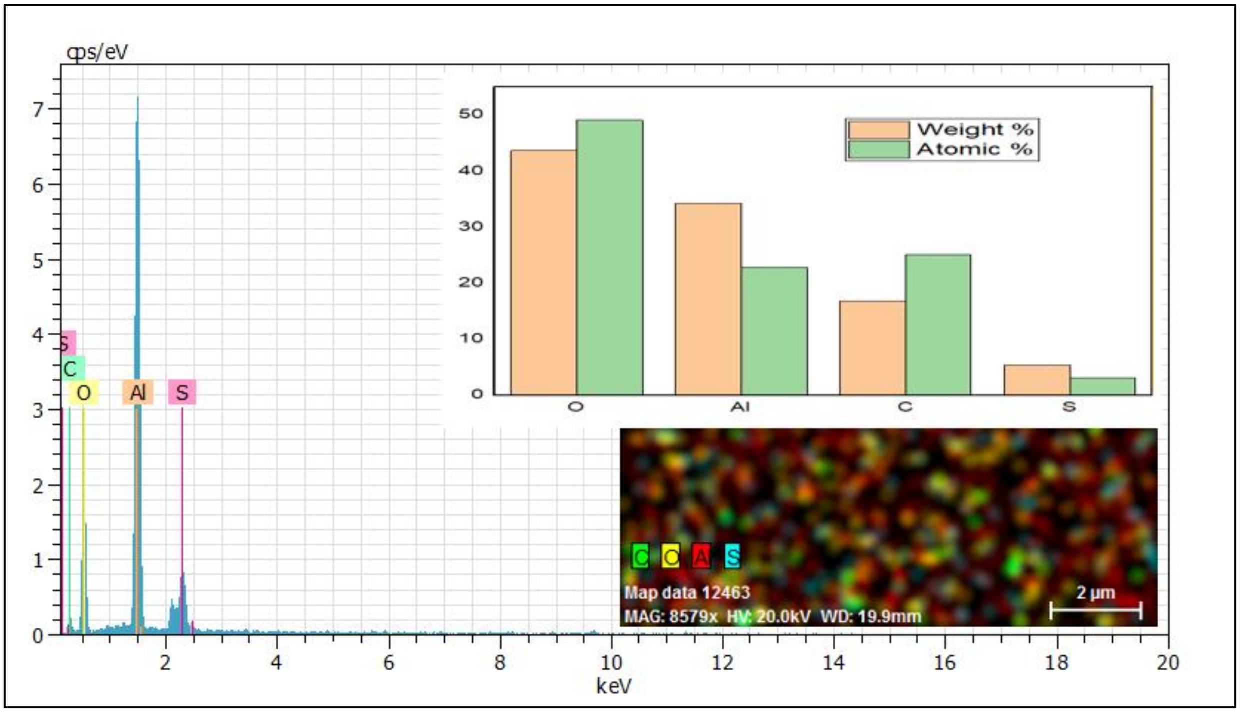

Figure -6: The chemical composition of the sample S4

Microstructure of the Anodized Layers

The surface morphology for the anodized layer can be shown by plan view SEM image in **Fig.7**, where the defects morphology, contaminants can be recognized. The surface countenances included the grain boundary grooves, surface imperfections (embedded particles, pores), and etching pits. The grain boundary grooves refer to the defect shape at the grain boundary, whereas the etching pits are cavities or surface scallops created due to varying etching behaviours between intermetallic inclusions or particles and the aluminium matrix[10], [11] . As seen in Fig. there are significant number of aggregated particles were presence at the anodized aluminium oxide layer surface, The grain boundaries are clearly visible on the anodized layer, at the same time it can be see clearly the surface defects, pores and surface scallops [12] . As reported in Murphy-Michelson model, after anodized oxide layer Al2O3 was formed, there are a part of aluminium oxide transferred from the layer surface into hydroxide by absorption of water, which led to renew the barrier layer on the metal side continuously. According to this model the formation of pores is essential for oxide formation, thus during anodization the anodized oxide layer is not separated from electrolyte onto carrier surface, but it's formed within outer layer transformation [13]. It can be noted that anodized oxide layer is formed on aluminum surface, and it composed of a porous film which agree with [14]. According to nucleation model, the anodized oxide formation does not homogenous on the surface, but a small solution nucleates appear spread at a specified point. The nucleation process occurs rapidly, homogenously, and continuously, in which these nuclei related on operation parameters such applied voltage and electrolyte concentration [15]. As can be seen in Fig. the microstructure of the surface is non homogenous and contains cavities. It can be noted that some of these cavities may be vanish via it was filled with corrosion products, while the others may be covered by oxide particles too [16].

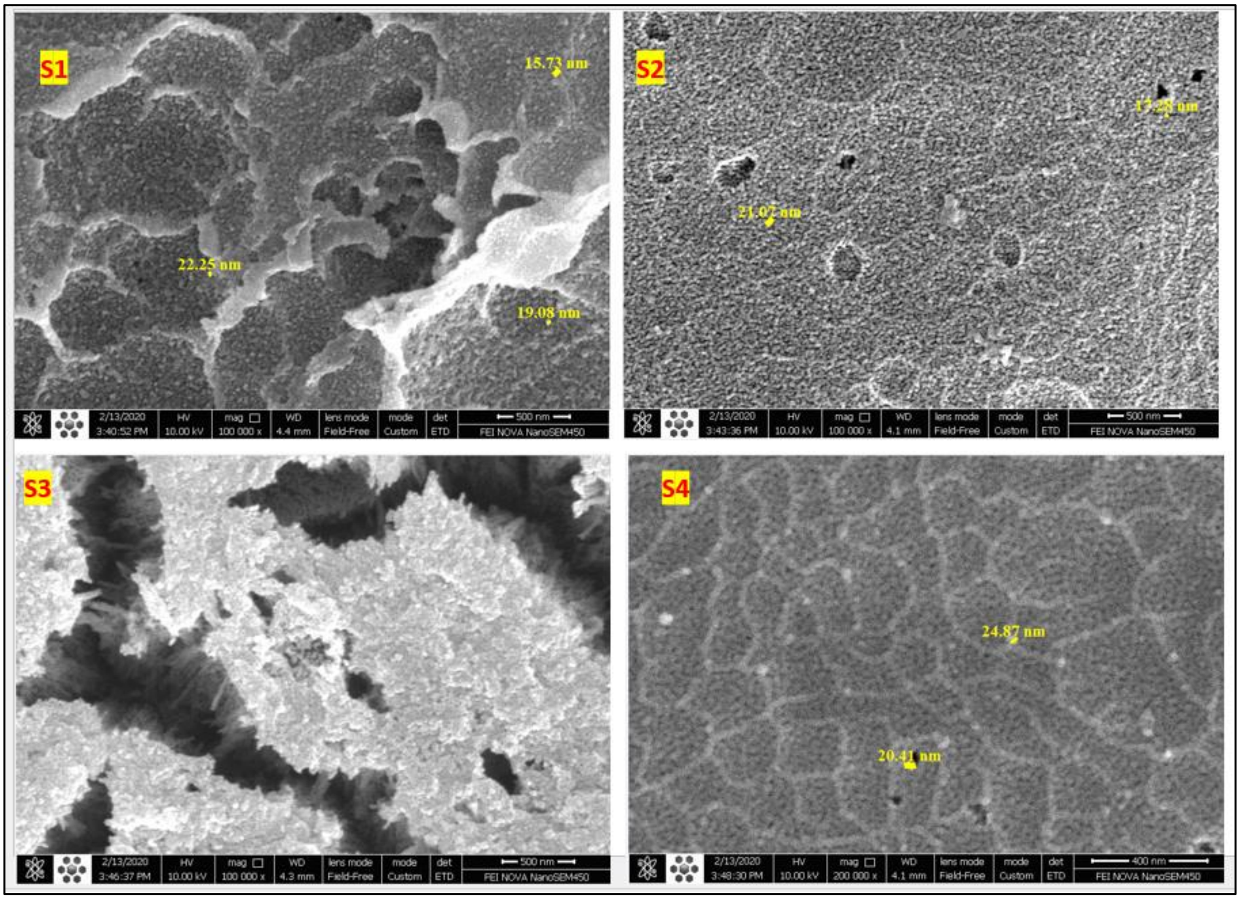

Figure -7: The SEM micrograph of the aluminium layer surface for four specimens

Weight gain calculation

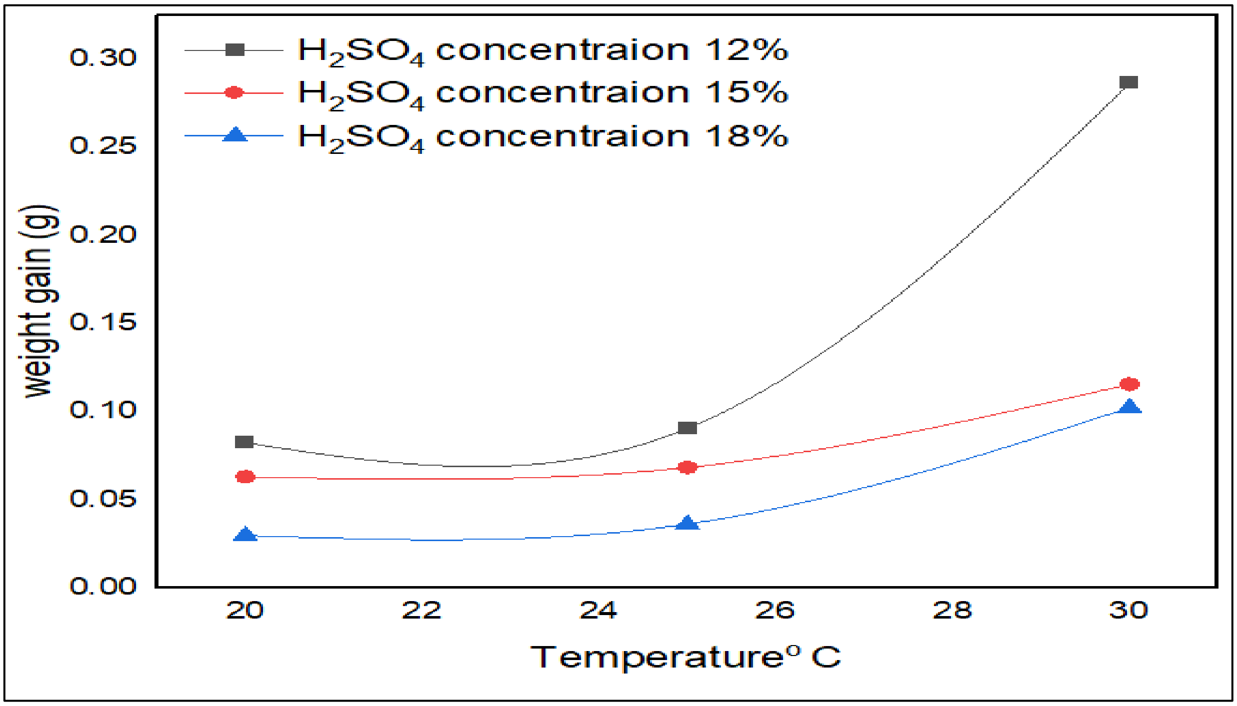

Figure -8: Weight gain as a function of temperature and acid concentration time 30 min, current density 2.5

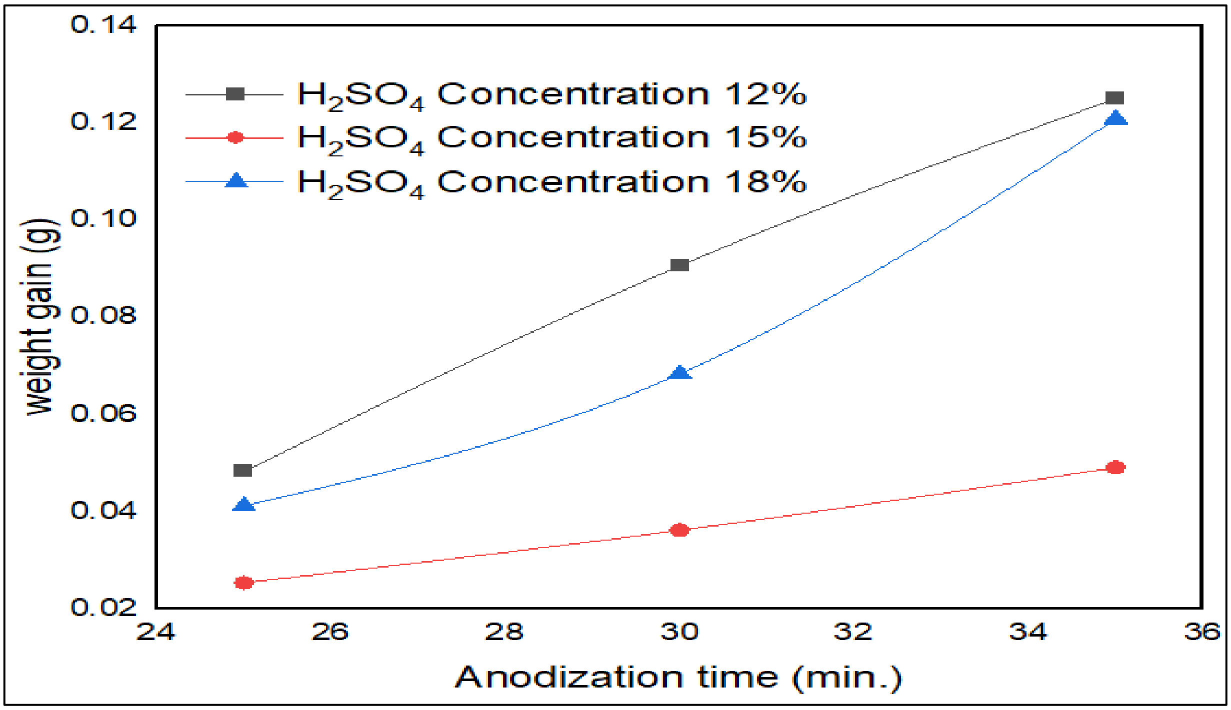

Figure -9: Weight gain as a function of temperature and acid concentration temp 25 , current density 2.5 .

The weight gain for was show in figures, in which the combine effect of anodization temperature and acid concentration shown in Figs 8-9. the weight gain increasing with temperature and decreasing with acid concentration increase, and this is because increasing in the rate chemical dissolution of anodized oxide layer. The weight gain of anodic oxide layer increases with increasing of anodization time as shown in Fig. because the increasing in the oxide layer formation is proportional to the electric charge according to Faraday's law but as the acid concentration increased the mass gain was decreases as chemical dissolution increases with acid concentration. The weight gain of anodic oxide layer is a result of competition between rate of chemical dissolution and the rate of oxide layer formation [17], [18].

Anodized layer thickness calculation

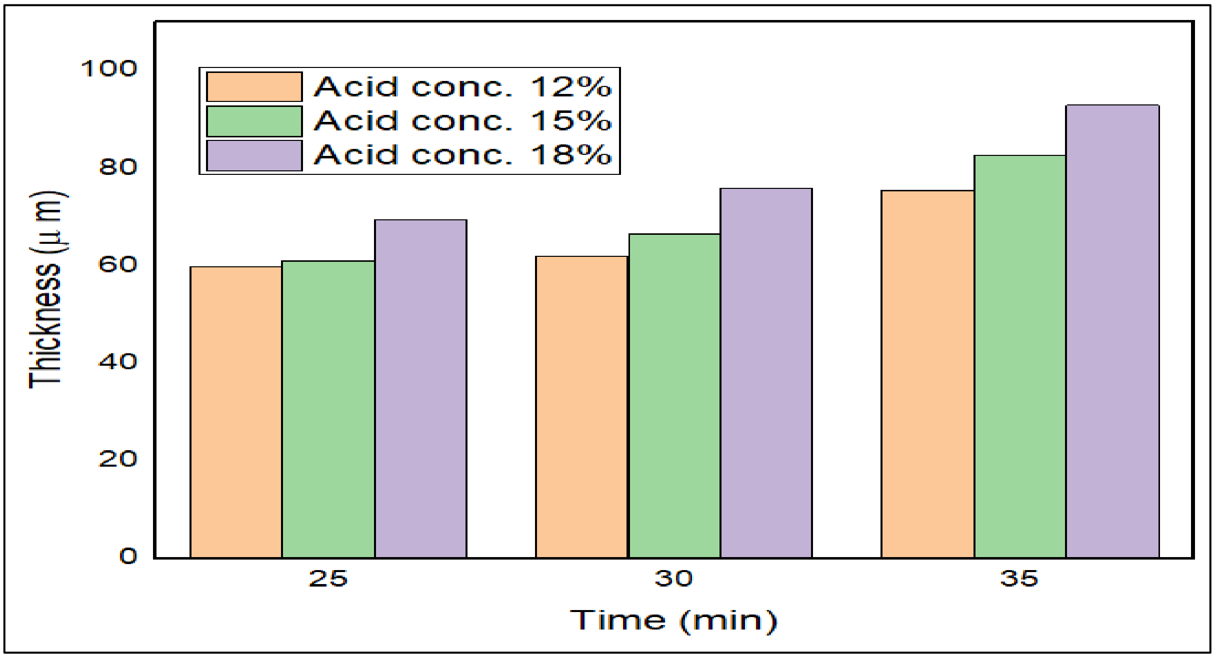

Figure -10: Impact of duration and acid concentration at a constant temperature of 25°C and a current of 2.5 A.

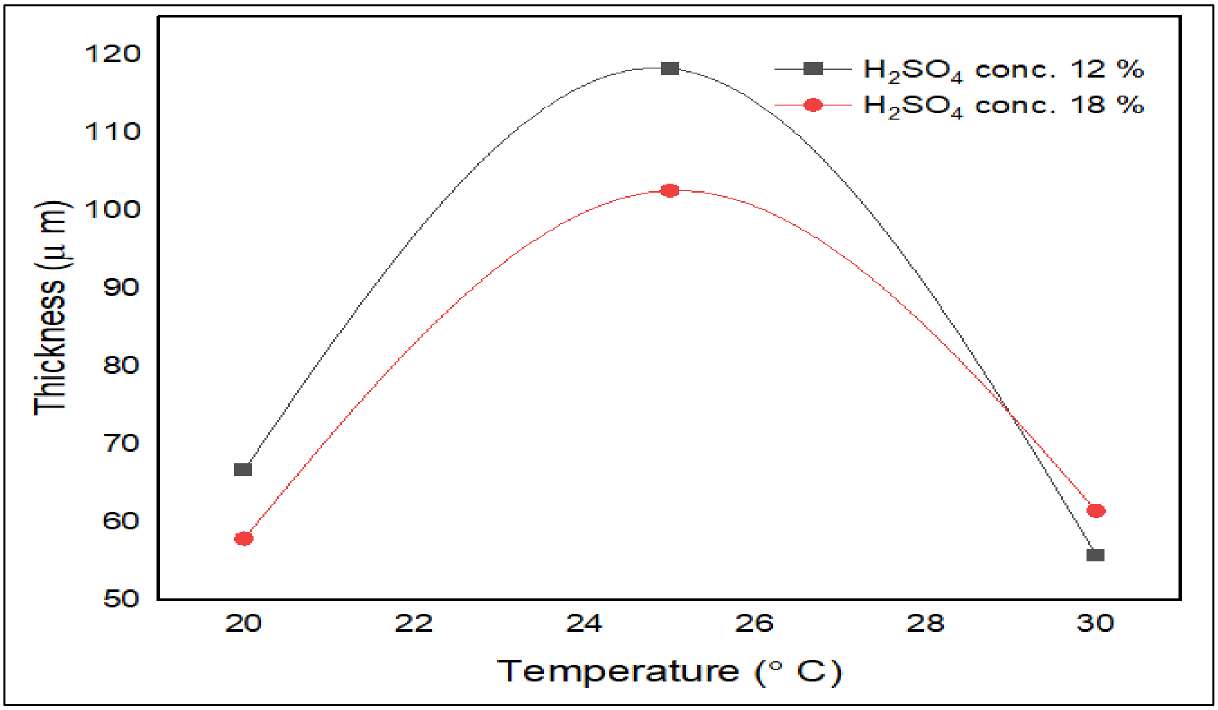

Figure -11: Impact of duration and acid concentration at a constant temperature of 25°C and a current of 2.5 A.

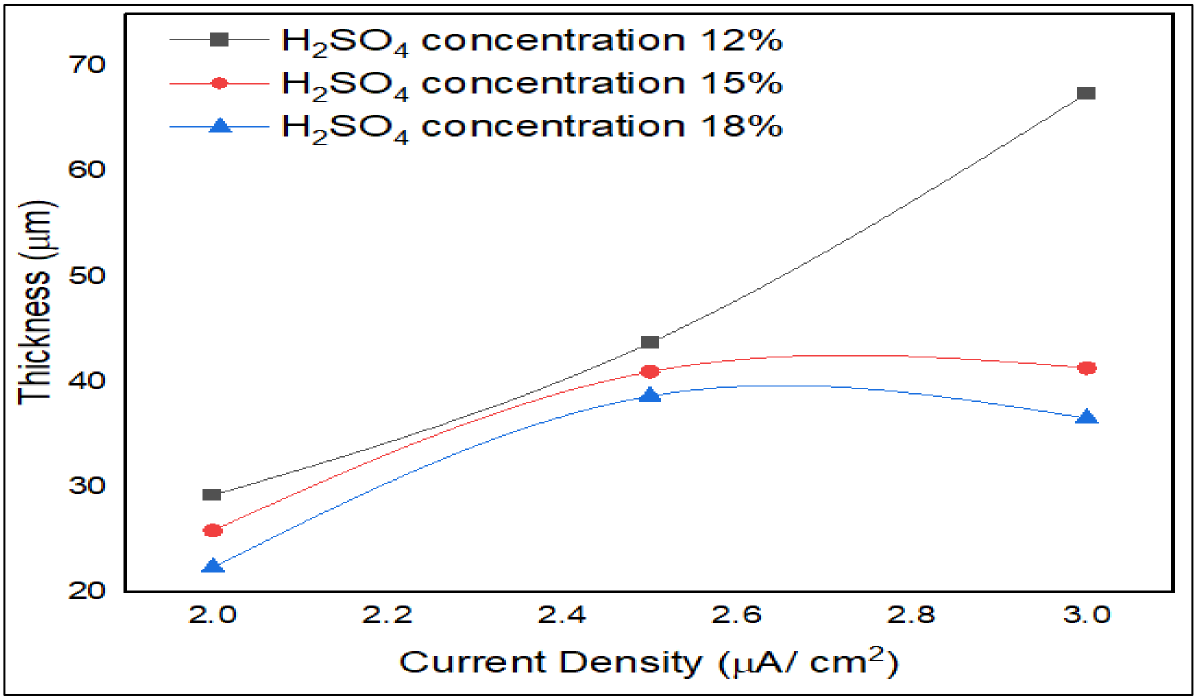

Figure -12: Impact of current and acid concentration at a constant temperature of 25°C throughout a duration of 30 minutes.

The thickness of anodized oxide layer is corresponded to about two times of actual thickness approximately and this is because of both side of aluminium species were anodized. Thickness is not increasing linearly with anodization time but reaches a limit, characteristic of the process. It may be concluded that thickness of anodic oxide layer can be related with quality, temperature, concentration and current conditions of the electrolyte solution. As noted in the above figures the thickness of formed layer is decreased with temperature in which the growth rate of layer is more at room temperature than at temperature above [19], while the thickness of this layer is proportional with applied current density via the increasing in electric charge according to Faraday's law [20]. It was noted that the increasing applied current produce thick and porous system because the using of high current destiny may be mean intensity in dissolution rate, leading to large pores formation [20].Again, and as it was mentioned above the oxide layer thickness is inverse proportional with electrolyte temperature due to increasing in dissolution rate by acidic media [21] , so the limiting of layer thickness because high rate of dissolution of oxide layer in sulfuric acid as well as at high temperature [22].

Conclusions

The present work investigated the effects of temperature, anodization time, electrolyte concentration, and current density on anodization of aluminium. The produced anodized oxide layer shows high O/Al ratio between 1.096 and 1.307 under different operation conditions. Weight gain was ranged between 0.0229 to 0.125 g under effect of temperature -time- concentration-current density in which the weight gain was increased with temperature and time but decreased with acid concentration. While the Aao thickness is ranged between 22.367 to 118.33 µm under effect of temperature -time- concentration-current density, whereas the thickness was increased with current density, acid concentration and time, but it decreased with temperature.

References

1. M. Mehdizade, A. R. Eivani, and M. Soltanieh, “Characterization of the anodic oxide layer deposited on severely deformed and aged AA6063 aluminum alloy,” *Journal of Materials Research and Technology*, vol. 15, pp. 68–85, 2021.
2. H. Uchi, T. Kanno, and R. S. Alwitt, “Structural features of crystalline anodic alumina films,” *J Electrochem Soc*, vol. 148, no. 1, p. B17, 2001.
3. A. Hakimizad, K. Raeissi, and F. Ashrafizadeh, “Characterization of aluminum anodized layers modified in sulfuric and phosphoric acid baths and their effect on conventional electrolytic coloring,” *Surf Coat Technol*, vol. 206, no. 8–9, pp. 2438–2445, 2012.
4. E. R. I. Mahmoud, A. Algahtani, S. Z. Khan, and G. M. S. Ahmed, “Characterizations of Cladded 6082-T6 Aluminum Alloy Through Hard Anodizing,” *Sci Adv Mater*, vol. 12, no. 7, pp. 1034–1045, 2020.
5. J. Lee, Y. Kim, H. Jang, and W. Chung, “Cr2O3 sealing of anodized aluminum alloy by heat treatment,” *Surf Coat Technol*, vol. 243, pp. 34–38, 2014.
6. I. Mohammadi, S. Ahmadi, and A. Afshar, “Effect of pulse current parameters on the mechanical and corrosion properties of anodized nanoporous aluminum coatings,” *Mater Chem Phys*, vol. 183, pp. 490–498, 2016.
7. A. W. Juyana and M. N. B. Derman, “Characterization of porous anodic aluminium oxide film on aluminium templates formed in anodizing process,” *Adv Mat Res*, vol. 173, pp. 55–60, 2011.
8. J. Gu, X. Zhang, and L. Yu, “Investigation on anodized 5052 aluminum alloy and its corrosion resistance in simulated acid rain,” *Int J Electrochem Sci*, vol. 18, no. 11, p. 100336, 2023, doi: https://doi.org/10.1016/j.ijoes.2023.100336.
9. I. Dobosz, “Influence of the anodization conditions and chemical treatment on the formation of alumina membranes with defined pore diameters,” *Journal of Porous Materials*, vol. 28, no. 4, pp. 1011–1022, 2021.
10. Y. Ma, X. Zhou, G. E. Thompson, J.-O. Nilsson, M. Gustavsson, and A. Crispin, “Origin of streaks on anodised aluminium alloy extrusions,” *Transactions of the IMF*, vol. 91, no. 1, pp. 11–16, Jan. 2013, doi: 10.1179/0020296712Z.00000000075.
11. H. Zhu, M. J. Couper, and A. K. Dahle, “Effect of process variables on the formation of streak defects on anodized aluminum extrusions: An overview,” 2012.
12. S. Feliu, M. J. Bartolomé, and J. A. González, “XPS characterization of porous and sealed anodic films on aluminum alloys,” *J Electrochem Soc*, vol. 154, no. 5, p. C241, 2007.
13. M. Pashchanka, “Conceptual progress for explaining and predicting self-organization on anodized aluminum surfaces,” *Nanomaterials*, vol. 11, no. 9, p. 2271, 2021.
14. Q. Wang and H. Li, “Study on anodic oxidation of 2099 aluminum lithium alloy and sealing treatment in environmental friendly solutions,” *Int J Electrochem Sci*, vol. 18, no. 7, p. 100186, 2023, doi: https://doi.org/10.1016/j.ijoes.2023.100186.
15. P. Csokan, “Nucleation mechanism in oxide formation during anodic oxidation of aluminum,” in *Advances in corrosion science and technology*, Springer, 1980, pp. 239–356.
16. J. J. Suay, E. Gimenez, T. Rodrıguez, K. Habbib, and J. J. Saura, “Characterization of anodized and sealed aluminium by EIS,” *Corros Sci*, vol. 45, no. 3, pp. 611–624, 2003.
17. J. S. L. Leach and P. Neufeld, “Pore structure in anodic Al2O3 films,” *Corros Sci*, vol. 9, no. 6, pp. 413-IN6, 1969.

18. K. Labisz, L. A. Dobrzański, and J. Konieczny, "Anodization of cast aluminium alloys produced by different casting methods," *Archives of Foundry Engineering*, vol. 8, no. 3, pp. 45–50, 2008.

19. A. Musza *et al.*, "Tribological Examination of Anodized Al-356 for Automotive Use. Coatings 2023, 13, 1642," 2023.

20. A. Musza, D. Ugi, Á. Vida, and N. Q. Chinh, "Study of Anodic Film's Surface and Hardness on A356 Aluminum Alloys, Using Scanning Electron Microscope and In-Situ Nanoindentation. Coatings 2022, 12, 1528," 2022, *s Note: MDPI stays neu-tral with regard to jurisdictional claims in ….*

21. W. Bensalah, K. Elleuch, M. Feki, M. Wery, and H. F. Ayedi, "Optimization of anodic layer properties on aluminium in mixed oxalic/sulphuric acid bath using statistical experimental methods," *Surf Coat Technol*, vol. 201, no. 18, pp. 7855–7864, 2007.

22. Y. Goueffon, L. Arurault, S. Fontorbes, C. Mabru, C. Tonon, and P. Guigue, "Chemical characteristics, mechanical and thermo-optical properties of black anodic films prepared on 7175 aluminium alloy for space applications," *Mater Chem Phys*, vol. 120, no. 2–3, pp. 636–642, 2010.